09,12,11

Distribution of Tb^{3+} and Eu^{3+} cations in the C-Gd_2O_3 lattice according to photoluminescence and far IR spectra

© V.V. Bakovets, I.P. Dolgovesova, T.D. Pivovarova, L.A. Sheludyakova

Nikolaev Institute of Inorganic Chemistry, Siberian Branch, Russian Academy of Sciences, Novosibirsk, Russia

E-mail: becambe@niic.nsc.ru

Received August 12, 2021
Revised August 12, 2021
Accepted August 20, 2021

In this work, we investigated the features of the photoluminescence of C-$Gd_{2(1-x)}Tb_xEu_xO_3$ luminophores at $x = 1.0$ and 2.5 mol%, which are associated with the distribution of Tb^{3+} and Eu^{3+} activator ions over the centrosymmetric C_{3i} and noncentrosymmetric C_2 positions of cations in the bixbyite lattice, as well as in the positions at the boundaries crystallites C_S. We studied the phase transformations of the samples, changes in the morphology of crystallites, photoluminescence spectra, and spectra of the far infrared region $50-600\,cm^{-1}$ with changes in the annealing modes of the initial products of the sol-gel synthesis $Gd_{2(1-x)}Tb_xEu_x(OH)_y(CO_3)_z \cdot n(H_2O)$ at temperatures of 900 and 1200°C in air and hydrogen. Correlations have been established between changes in the characteristics of the samples and the parameters of their annealing. Based on the analysis of these correlations, the redistribution of activators over the indicated cation positions was determined, and a model was proposed for identifying infrared absorption bands in accordance with the localization of activators along the cationic sublattices C_{3i} and C_2.

Keywords: Gd oxide, luminescence activators Tb^{3+} and Eu^{3+}, annealing in air and in hydrogen, correlation of photoluminescence and far infrared spectra, distribution of activators in the lattice.

DOI: 10.21883/PSS.2022.14.54344.189

1. Introduction

Binary activation of a matrix of C-Gd_2O_3 with Tb^{3+} and Eu^{3+} ions expands opportunities of regulation in a wide range of luminescence tones of luminophores of various technical applications, particularly, for solving a problem of „warm-cold“ color [1,2]. In terms of physical chemistry of solids, study of changes of such luminophores emission spectra results in understanding of structure of a crystal lattice short- and long-range orders, particularly, distribution of cations-activators over the crystal sublattices of a complex compound. In the work [3] the features of phase transitions of solid solutions of $Gd_{2(1-x)}Tb_xEu_xO_3$ at annealing temperature change of hydrated products of sol-gel synthesis of $Gd_{2(1-x)}Tb_xEu_x(OH)_y(CO_3)_z \cdot n(H_2O)$ and concentration of luminescence activators of 1.0 and 2.5 mol% were examined. Changes of photoluminescence (PL) spectra with phase composition change were established.

The feature of luminophore matrices of sesquioxides of REE cubic modification is two types of Ln^{3+} ions distribution over cation sites of the crystal lattice of bixbyite type: centrosymmetric C_{3i} and noncentrosymmetric C_2 [4–6]. It is known, that equilibrium ratio of sites in a lattice cell is 8 cations in position C_{3i} and 24 cations in position C_2. Distribution of Eu^{3+} ions of FL activator in real materials, i.e. in materials, obtained under certain modes of chemical synthesis, heat processing and chemical composition of products, usually described with so called asymmetric ratio (AR) of intensity of the bands of $I_{C_2}/I_{C_{3i}}$ FL cations in positions C_2 and C_{3i}, which value can change within 2.8–12.0 [6,7]. AR change limits are related to concentration redistribution of activator over the lattice sites at increased sensitivity of radiative transition $^5D_0 \rightarrow {}^7F_2$ of Eu^{3+} ions in noncentrosymmetric site to change of a symmetry of their closest surrounding with ions of $[(O^{2-})_6 + 2O^{2-}]$. Another situation exists relative to Tb^{3+} cations distribution over the specified positions, since there are no reasonably substantiated rules of these ions FL spectra change in the specified positions. However, it is noted, that FL of Tb^{3+} cations is very sensitive to surrounding nature [8]. Therefore, thy electrons radiative transitions response to the closest surrounding crystal field change is rather strong. It is also known, that at increased concentrations of two FL activators the excitation energy of electrons optical transitions can be transferred from one activator to another [9]. It changes the relative intensity of both activators FL bands and, as a result, changes the perceived color of luminophore. The most probable transfer of excitation energy happens at equal concentrations of activators. At the same time, the most effective emission at 543 nm of Tb^{3+} cations happens at their concentration of 2.5 mol%. But there are other data, indicating the increased efficiency of Eu^{3+} ions FL at small concentrations of 0.0025–0.0050 mol% of Tb^{3+} ions [1,9,10].

Conditions of annealing of intermediate synthesis product of $Gd_{2(1-x)}Tb_xEu_x(OH)_y(CO_3)_z \cdot n(H_2O)$ also change the concentration of FL of Tb^{3+} activator, since annealing

in air results in oxidation of these ions to Tb^{4+} [11]. Whereby, above 600 and up to 1150°C the phase of variable composition of Tb_xO_y forms, while concentration of Tb^{4+} reduces due to non-sufficient oxygen pressure in air for maintaining the constant composition of a solid phase at increased temperatures. Besides, the examined materials are represented with polycrystalline nanostructured samples, which have a developed specific surface of crystallites [12]. The corresponding surface and boundary layers of crystallites contain about $10^{21}-10^{22}\,cm^3$ atoms with deformed short-range order of surrounding at crystallites size d_{cr} of about 50−150 nm. These surface layers also contain FL activators of Tb^{3+} and Eu^{3+}. It is obvious, that cations surrounding geometry in surface positions C_S will differ from symmetry of positions C_2 and C_{3i}. For instance, the FL bands broadening [13] indicate, that due to disruption of the system thermodynamic equilibrium the Eu^{3+} cations are coming out of the octahedral surrounding in volume of C-$Y_2O_3:Eu^{3+}$ to crystallites surface. As a result, FL activator in surface and boundary layers is under exposure of various crystalline fields of surrounding.

The most available methods of studying the changes of crystalline fields around cations of FL activators are methods of optical spectroscopy and, particularly, far infrared spectroscopy (FIR). It is known, that as per transition selection rules the Raman spectrum can not contain the bands of combinational scattering of molecular groups with centrosymmetric cation position, but in FIR spectra the absorption bands for both cation positions C_{3i} and C_2 [13] are allowed. Work [14] includes justification of the fact, that in FIR spectra of cubic C-Eu_2O_3 and C-$Y_2O_3:Eu^{3+}$ the absorption bands 130 ± 5 and $200 \pm 2\,cm^{-1}$ describe cations vibrations in positions C_{3i} and C_2 respectively.

At high temperatures the cubic modification of REE sesquioxides can transition into monoclinic B-Ln_2O_3 [15] that in presence of FL activators should result in radiation spectrum change due to lack of positions C_{3i} in the lattice.

In accordance with the above mentioned, the purpose of this work is to study changes of Tb^{3+} and Eu^{3+} FL activators distribution over cation sites C_{3i}, C_2 of the crystal lattice and sites C_S depending on temperature and annealing atmosphere of products of sol-gel synthesis of $Gd_{2(1-x)}Tb_xEu_x(OH)_z(CO_3)_z \cdot n(H_2O)$, chemical composition of solid solutions C-$Gd_{2(1-x)}Tb_xEu_xO_3$ and coexisting phases, as well as on nanomorphology of powders based on analysis of spectra of FL and FIR spectroscopy.

2. Experimental part

Sol-gel method [3] was used to obtain the solid solution compounds of $Gd_{2(1-x)}O_3:(Tb^{3+,4+})_x(Eu^{3+})_x$. Nitrates of $Gd(NO_3)_3 \cdot 6H_2O$, $Tb(NO_3)_3 \cdot 5H_2O$ and $Eu(NO_3)_3 \cdot 5H_2O$, obtained from the corresponding oxides, with the main component content of at least 99.9% were used as reagents in the work. Two-fold excess of NaOH solution of „extra pure“ grade in double-distilled water was used as a precipitator. The synthesis was performed at a setup with initial reagents spraying for homogeneity achieving in the work solution volume. The obtained sediment of $Gd_{2(1-x)}Tb_xEu_x(OH)_y(CO_3)_z \cdot n(H_2O)$ was cleaned to neutral pH value of wash waters and dried in air at 50°C. Then the samples were annealed at 900 and 1200°C for 1−2 h until formation of the end products — solid solutions of $Gd_{2(1-x)}O_3:(Tb^{3+,4+})_x(Eu^{3+})_x$ at total absence of water as per IR spectroscopy. Detailed information on synthesis technique and justification of activators concentration selection, as well as details of X-ray phase analysis and FL spectroscopy are presented in the work [3]. FIR spectra were registered using VERTEX 80v spectrometer with spectral resolution of $0.2\,cm^{-1}$. Powder samples were crushed with PE-spectral polyethylene and tablets were made by compression. Registration of FIR spectra was performed in pure dry nitrogen atmosphere.

3. Results and discussion

3.1. Nanomorphology, phase composition, FL and FIR spectra of samples

Table contains annealing temperature and atmosphere of the samples, their phase composition as per data of X-ray phase analysis and average size of crystallites d_{cr} as per calculation using Debye−Scherrer model. Samples № 4 and 8 are products of additional annealing in hydrogen of samples № 3 and 7 respectively. Samples 1 and 2 [3] are not examined, since they contain carbonate and hydrate forms annealing products at 700°C. Sample 6, obtained by annealing of sample 5 in H_2, was not examined, since it was presented mainly by monoclinic modification of B-$Gd_2O_3:Tb^{3+}$, Eu^{3+}, which lattice does not have centrosymmetric sites of cations and impurity phase of Tb_7O_{12}. Therefore, hereinafter this sample will be mentioned only in case of necessity. Unlike the earlier presented data [3], in this work the values of FL bands intensities I_{FL} and their ratios $I_{\lambda_1}/I_{\lambda_2}$ are presented with rounding to two decimal places, that does not exceed the experimental errors of 5 and 10%, respectively, but is required for more detailed analysis of the further results.

Coexisting phases of Tb_7O_{12} compounds (trigonal, *sp. gr.* $R\bar{3}$, ICSD 73822) and $TbO_{1.81}$ (cubic, *sp. gr.* $Fm\bar{3}m$, ICSD 28916) have 50 and 100% cationic C_{3i} sites in the lattice structure respectively, but these phases content level does not exceed 1−2% [3].

Figure 1 shows dependencies of changes of crystallites sizes and hypothetic specific surface area S_{cr} of crystallites. It is obvious, that crystallites size increases with temperature growth at repeated annealing in hydrogen and slightly decreases at FL activators concentration increase to 2.5 mol%. Change of specific surface of crystallites, according to geometric representations, is mirrorlike to a change of d_{cr} value. Quantitative model calculations of S_{cr} values are presented in the work [12].

Phase composition, annealing temperature, samples annealing atmosphere, crystallites size d_{cr}, regions of change of maximums λ_{FL}, FL bands and their average values $\lambda_{FL,middle}$, intensity I_{FL} of FL bands and their ratios $I_{\lambda_1}/I_{\lambda_2}$

Sample № (initial sample)		3 (sol-gel product)	4 (sample 3)	5 (sol-gel	7 (sol-gel product)	8 (sample 7)
Annealing temperature, °C		900°C		1200°C		
Annealing atmosphere		Air	H_2	Air	Air	H_2
Phases		C-Gd_2O_3 Tb_7O_{12} $TbO_{1.81}$	C-Gd_2O_3	C-Gd_2O_3 Tb_7O_{12}	C-Gd_2O_3	C-Gd_2O_3
d_{cr}, nm		35	80	> 170	120	150
λ_{FL}, range, nm	λ_{FL}, middle, nm	Photoluminescence bands intensity, I_{FL}, Relative units				
610–614	612	2.04	4.01	10.59	10.48	24.04
594–595	595	0.52	1.54	4.04	2.15	4.96
550–552	551	2.04	7.03	16.75	7.23	18.78
541–547	545	2.55	7.95	18.58	7.34	22.03
490–495	492	1.02	4.99	9.04	3.03	9.75
λ_1/λ_2, nm		Ratios of bands intensity FL, $I_{\lambda_1}/I_{\lambda_2}$				
612/595		3.92	2.60	2.62	4.87	4.85
492/551		0.50	0.71	0.49	0.42	0.51
492/545		0.40	0.63	0.49	0.41	0.44

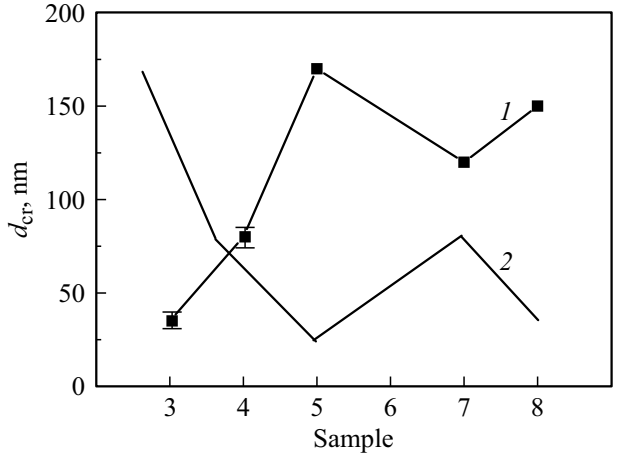

Figure 1. Crystallites size d_{cr} (*1*) and hypothetic specific area of crystallites boundaries (*2*) of samples 3–8.

Table includes FL bands intensities in relative units after normalization of all spectra by reference sample spectrum of C-$Y_2O_3:Eu^{3+}$ (3 mol%). According to the table, intensity of the main FL bands of Eu^{3+} and Tb^{3+} activators: increases with increase of annealing temperature of products of sol-gel synthesis in air and at additional annealing in hydrogen. Intensity slightly changes for the band 612 nm, significantly drops for the band 595 nm of Eu^{3+} ions, strongly drops for doublet of the bands 551, 545 nm and for the band 492 nm of Tb^{3+} ions at increase of Eu^{3+} and Tb^{3+} concentration from 1.0 mol% (samples 3–5) to 2.5 mol% (samples 7 and 8).

Figure 2 shows FIR spectra of samples of C-$Gd_2O_3:Tb_x,Eu_x$ ($x = 1.0$ and 2.5 mol%). Real spectra have strongly curved base line, therefore the figures contain spectra, reduced to a straight horizontal base line. Strong curving of a background base line was also observed earlier for cubic sesquioxides of REE [14,16], that is related to a lattice phonon absorption and light flow scattering in this region of the spectrum. For samples 3 and 4, annealed at 900°C, the peaks are rather narrow, that is characteristic for perfect crystal lattices of sesquioxides of REE [17]. At annealing temperature of 1200°C for samples 5, 7 and 8 the bands become wider, thus indicating the appearing the disruptions of the short-range order lattices.

FIR spectra of all samples can be divided into three theoretical groups: small 100–250 cm^{-1} (A), medium 250–400 cm^{-1} (B) and large 400–600 cm^{-1} wave numbers (C). Additional absorption appears at the band 111 cm^{-1}. Similar, but much weaker band appears for Eu_2O_3 and Gd_2O_3. This absorption was attributed earlier to a local mode, created by impurity, e.g. Sm^{3+}, common for these three oxides [14]. But Sm^{3+} has intensive FL band of 650 nm, that was not observed in our case [3]. Group A represents vibrational modes F_u of Eu^{3+}, Gd^{3+}, Tb^{3+} cations [14,18], group B — torsion and deformation vibrations [18,19], including oxygen ions motion [14] and the band 500–550 cm^{-1} — valence vibrations of Ln–O bonds [18,20]. Absorptions below 90 cm^{-1} are related to electron excitation [14]. It can

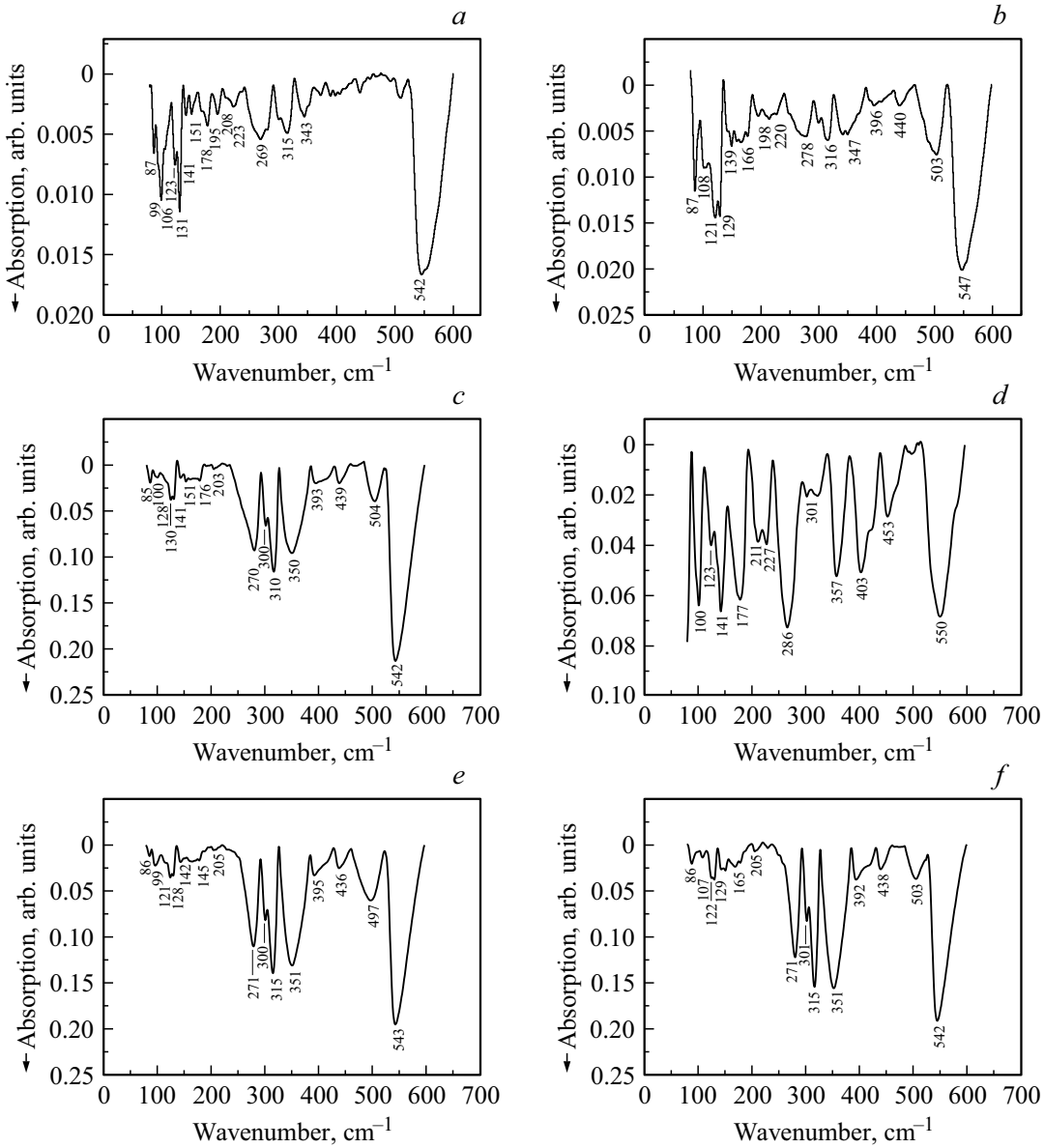

Figure 2. FIR spectra of $Gd_2O_3:Tb_x,Eu_x$: samples 3, 4, 5 and 6 ($x = 1.0$ mol%), annealing at 900°C: sample 3 in air (*a*), sample 4 in hydrogen (*b*); annealing at 1200°C: sample 5 in air (*c*), sample 6 in hydrogen (*d*); annealing at 1200°C, samples 7 and 8 ($x = 2.5$ mol%) in air (*e*), in hydrogen (*f*).

be assumed, that motions of various rare earth elements are weakly connected, at least in cationic sites C_{3i} (region of 120–145 cm^{-1}), since the spectra demonstrate narrow bands at small wave numbers. This fact allows to assume, that these motions have local resonance modes nature [14]. For cationic sites C_2 the larger overlap of absorption bands and their larger width are characteristic. It is characteristic, that spectrum of C-Gd_2O_3 in the work [17] has a doublet of absorption bands 124 and 130 cm^{-1}, that corresponds to spectrum region of cations of Eu^{3+} 130 cm^{-1} in C-Y_2O_3 matrix in site C_{3i} [14]. Triads of closely-located bands in a region of 120–145 cm^{-1} are observed. Considering FIR bands shift towards small wave numbers region by sesquioxides series of Tb → Gd → Eu [16], it is, probably, more correct to attribute (by average values for all samples) the band ~ 122 cm^{-1} to vibrations of Eu^{3+} ions, and the band ~ 130 cm^{-1} to vibrations of Gd^{3+} ions. Recovery of Tb^{4+} ions to Tb^{3+} after annealing at 900°C in hydrogen (sample 4) appears as significantly higher intensity of the band ~ 141 cm^{-1} relative to this band for sample 3. Then the band ~ 141 cm^{-1} can be attributed to Tb^{3+} ions motion. The specified shift of FIR absorption bands is defined with REE masses ratio. In a similar way, sites C_2 of cations can be attributed to absorption bands triad: ~ 192 to Eu^{3+} ions, ~ 208 to Gd^{3+} ions and ~ 226 cm^{-1} to Tb^{3+} ions. It should be noted, that Gd^{3+} cations belong to matrix, therefore have the highest concentration. At the same time, intensity of the absorption band 130 cm^{-1}, related in our opinion to motion

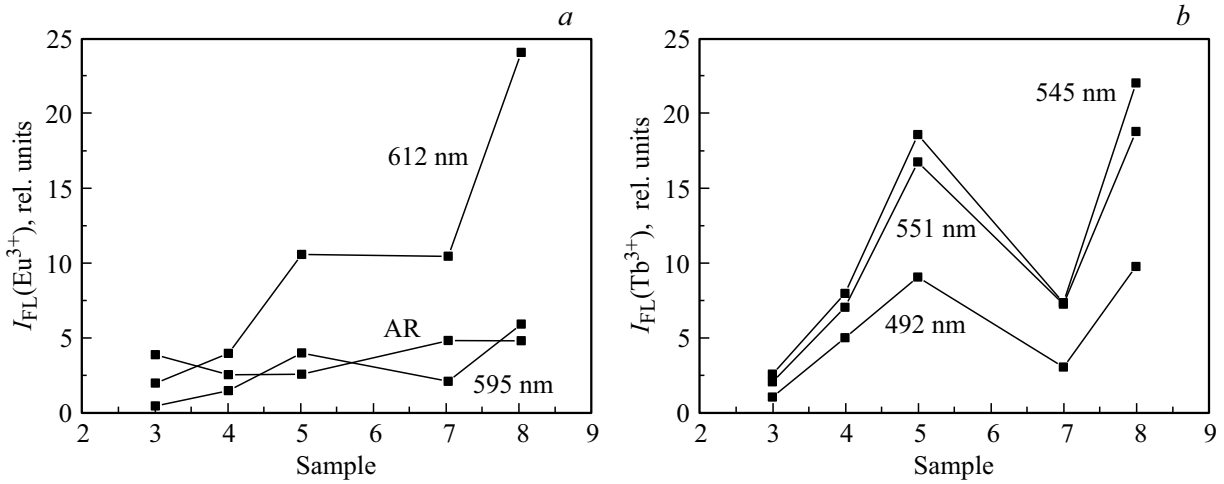

Figure 3. Intensity I_{FL} of the main bands of FL activators of ions of Eu^{3+} and AR (*a*) and Tb^{3+} (*b*).

of Gd^{3+} cations, is comparable with intensity of the bands of Eu^{3+} and Tb^{3+} impurity cations.

For free ions of Gd^{3+} the special electron configuration in REE range with orbital magnetic moment of $L = 0$ is characteristic. This is, probably, appears as weak intensity of FIR absorption bands in surrounding sphere, close to octahedral. It seems, the bands 130 and 208 cm^{-1} represent motion of Gd^{3+} cations only, for which the second surrounding sphere has activators cations, resulting in significant disruption of crystal field symmetry and appearance of significant dipole moment. It is obvious, that concentration of such Gd^{3+} ions is comparable with concentrations of FL activators.

3.2. Analysis of distribution of Eu^{3+}, Tb^{3+} and Gd^{3+} cations in positions C_{3i}, C_2, C_S by crystallites nanomorphology and FL and FIR spectra of the samples

According to Fig. 1, sample 3 annealing in hydrogen at 900°C (sample 4) is accompanied with increase of crystallites size d_{cr}. Therefore, the specific area S_{cr} of crystallites boundaries reduces [12]. This is accompanied with reduction of Tb^{4+} ions to Tb^{3+} and their primary departure from sites C_S in crystallites volume, preferably to sites C_{3i} due to lowest cation radius in series of $Eu^{3+} \leq Gd^{3+} > Tb^{3+}$ [3]. Besides, concentration of Tb^{3+} ions increases due to reducing ions of Tb^{4+}, also presented in crystallites volume.

Figure 3 shows dependencies of intensity changes of the main FL bands of Eu^{3+} and Tb^{3+} activators of samples 3–8. FL bands intensity of Eu^{3+} ions increases: I_{612} in 2 times and I_{595} in 3 times (Fig. 3, *a, b*) due to increase of a sample crystallinity degree and increase of excitation energy transfer of Tb^{3+} ions to Eu^{3+} ions with growth of reducing Tb^{3+} ions concentration. At the same time, AR decreases to 2.7 — almost equilibrium value of 3. Intensity of all FL bands of Tb^{3+} ions grows due to increase of samples crystallinity and concentration growth of these ions, but I_{492} increases less than others. It is obvious, that short-range order structure changed at annealing, and this should be represented in FIR spectra.

Figure 4, *a, b* shows dependencies of FIR absorption bands intensities for cations of Eu^{3+}, Gd^{3+} and Tb^{3+} in sites C_2 and C_{3i} according to spectra, presented in Fig. 2.

Attempt to normalize these values by maximum absorption band 545 cm^{-1}, presenting superposition of all cations bands for Ln–O bond, that could be taken as a constant value for all samples, failed. The obtained dependencies assured us that these bands can not be used as reference, since a change of FIR incident light flux scattering happens at significant change of polycrystalline samples crystallites size at transition from samples 3, 4 to samples 5, 7, 8 (Fig. 2). Besides, this scattering degree changes for each sample at FIR incident light flux spectrum transition from region A to regions B and C.

As per Fig. 4, at transition from sample 3 to sample 4 the intensity of FIR absorption bands of Tb^{3+} and Eu^{3+} cations insignificantly reduces in site C_2 and increases in position C_{3i}. This corresponds to transition of some of these cations from sites C_S to sites C_{3i} at reduction of S_{cr} and at increase of Tb^{3+} ions concentration due to reducing of Tb^{4+} ions.

All these factors combining, considering the data presented in the next paragraph, yields the conclusion on increased transfer of part of the energy of doublet 551, 545 nm of Tb^{3+} to excitation of FL band 595 nm of $(Eu^{3+})_{C_{3i}}$ ions by series of transitions $^5D_4(Tb^{3+})_{C_{3i}} \rightarrow {}^5D_1(Eu^{3+})_{C_{3i}} \rightarrow {}^5D_0(Eu^{3+})_{C_{3i}}$. At the same time, considering rather high symmetry and long-range order degree of the lattice as per data of *X*-ray phase analysis, the excitation transfer is performed exactly over C_{3i} sublattice. The basis for the made conclusions in this case is an assumption on increased probability of excitation transfer exactly through the abovementioned channel with the following radiative transition of $^5D_0(Eu^{3+})_{C_{3i}} \rightarrow {}^7F_1(Eu^{3+})_{C_{3i}}$

at exceeding the maximum allowable level population of the radiative transition of ${}^5D_{4,C_{3i}} \rightarrow {}^7F_{5,C_{3i}}$ of Tb^{3+} cations (doublet of the bands 551, 545 nm). In elaboration of the presented description of FL processes in this system we can assume, that the second by intensity FL band 492 nm belongs to $(Tb^{3+})_{C_2}$ ions, located in noncentrosymmetric C_2 cation site of the lattice.

Using the presented analysis algorithm, we can describe the features of Tb^{3+} and Eu^{3+} activators distribution in C-Gd_2O_3 lattice of sample 5, which is a product of annealing of hydrated product of sol-gel synthesis in air at 1200°C. Crystallites size is significantly bigger compared to sample 3 crystallites, Tb^{3+} ions concentration in crystallites volume is higher due to lower population of site C_S with these cations, that have a property of crystallites growing inhibitor. Besides, less oxygenated Tb^{4+} ions form at significantly lower partial pressure of O_2 in air atmosphere at higher annealing temperature relative to equilibrium value [11]. It is possible, that larger part of Tb^{4+} ions is in impurity phase of Tb_7O_{12} (see the table). Since intensity of FL band 492 nm of Tb^{3+} ions increased in 9 times, which is the most, and intensity of the band 612 nm of Eu^{3+} increased much higher relative to sample 3 than intensity of the band 595 nm, the excitation energy transfer to $(Eu^{3+})_{C_2}$ ions from Tb^{3+} ions happened over sublattice of C_2 sites. This is also based on effect of Tb^{3+} ions excitation population excess at transition $({}^5D_4)_{C_2} \rightarrow ({}^7F_6)_{C_2}$. Then this excess of excitation energy is transferred through transitions ${}^5D_4(Tb^{3+})_{C_2} \rightarrow {}^5D_1(Eu^{3+})_{C_2} \rightarrow {}^5D_0(Eu^{3+})_{C_2} \rightarrow {}^7F_2(Eu^{3+})_{C_2}$. While AR remains close to equilibrium value of 2.8. Therefore, in this case also the band 492 nm belongs to site C_2 of Tb^{3+} ions, while doublet of the bands 551, 545 nm belongs to C_{3i} position of cation.

At formation of sample 5 the intensity of FIR absorption bands of Tb^{3+} and Eu^{3+} cations is significantly lower in site C_2 and significantly higher in site C_{3i} (Fig. 4). This corresponds to transfer of most of these cations from sites C_S at significant reduction of S_{cr}. Besides, Tb^{3+} ions concentration is higher at oxidation of less ions under conditions of relatively lower oxygen pressure in air atmosphere, required for maintaining the oxygen excess in solid phase of C-$Gd_2O_3:Tb_x, Eu_x$ at higher temperature.

For sample 7 with Tb^{3+} and Eu^{3+} activators concentration of 2.5 mol%, obtained by annealing of hydrated product of sol-gel synthesis and annealed at 1200°C, the crystallites size is significantly less than for sample 5 (Fig. 1). This is associated with increase of Tb^{3+} ions concentration, including at crystallites boundaries, where they act as a surface-active inhibitor of crystallites growth [3]. At the same time, at annealing in air, the terbium ions, coming out of crystallites volume to their boundaries, will be represented with oxygenated form of Tb^{4+}. These cations concentration is probably low due to small oxygen pressure in air, so they are only at crystallites boundaries. Indeed, X-ray phase analysis did not register the phases, different from phase of C-Gd_2O_3, characterizing with oxygen excess, e.g. Tb_7O_{12} or $TbO_{1.81}$. Intensity of FL band 612 nm of $(Eu^{3+})_{C_2}$ did not change, while of the band 595 nm of $(Eu^{3+})_{C_{3i}}$ reduced in half compared to this parameter for sample 5. At the same time, intensities of the doublet bands 551, 545 nm of Tb^{3+} ions reduced almost the same. Thus, reduction of I_{595} value of FL ions of $Eu^{3+}(C_{3i})$ confirms transfer of FL excitation of these bands over C_{3i} sublattice from electron level of ${}^5D_4(Tb^{3+})_{C_{3i}}$. Since it is known [9], that at concentrations of FL activator of Tb^{3+} in $CaWO_4$ and Y_2O_3 matrices above 1.5 mol% the FL suppression starts to appear due to change interactions of activators ions, it is possible, that such FL suppression processes also happen in Gd_2O_3 matrix, especially for Tb^{3+} ions. Indeed, the sample crystallinity degree is less than for sample 5, and intensity of FL band 612 nm of Eu^{3+} ions remains unchanged, while concentration of Eu^{3+} ions in crystallites volume increases due to Tb^{3+} ions coming out of crystallites boundaries. Probably, the suppression effects are transferred over the both sublattices, but weaker over cations sublattice in noncentrosymmetric site C_2, that was observed in the work [9].

In support of FL suppression effects, especially for Tb^{3+} ions, the FIR spectra (Fig. 4) demonstrate significantly higher concentration of these ions relative to sample 5. This corresponds to increase of total concentration of Tb^{3+} ions to 2.5 mol%. At the same time, it is possible, that small level of concentration of ions of Eu^{3+} $(I_{FIR})_{Eu^{3+},C_{3i}} \approx$ const in site C_{3i} is compensated by a growth of these ions concentration in site C_2 ($(I_{FIR})_{Eu^{3+},C_2}$ increased by 0.005 Rel. units) (Fig. 4).

Additional annealing of sample 7 in hydrogen at 1200°C (sample 8) results in increase of crystallites sizes d_{cr}. Similar to the previous reasoning, Tb^{4+} ions at crystallites boundary surface of sample 7 are reduced to Tb^{3+} and transfer from surface sites C_S to site C_{3i} of C-Gd_2O_3 matrix. Intensity of all FL bands increased for both activators. However, in this case the intensity of FL band 622 nm strongly increased, that was also observed at formation of monoclinic modification of B-$Gd_2O_3:Tb_x, Eu_x$ [3]. This is because the annealing temperature of 1200°C is close to Tamman temperature, resulting the crystal lattice loosening due to development of atoms mobility [21]. At the same time, the crystal lattice reaches a labile state relative to reconfiguration into monoclinic modification. This fact is confirmed with decrease of the lattice parameter to 10.7958(2) Å against the value of 10.8040(2) Å for sample 7 [3], and, as known, the ratio of volumes of the lattice cells $V_M/V_C = 1263/436$ (ICSD 184528 and ICSD 96207) is such, that there are 72.666 Å^3 and 78.995 Å^3 per a single formula unit respectively. Therefore, the crystal lattice tightens at transition to monoclinic modification. Indeed, the additional annealing of the samples in Ar and H_2 (sample 6) [3] at temperature of 1200°C results in monoclinic phase formation, that is expected from thermodynamic properties of REE oxides [15]. Therefore, for sample 7 the symmetry of sites C_{3i} (short-range order of the lattice) is significantly deformed, and differentiation of cations states in sites C_{3i}, C_2 and C_S using optical spectroscopy methods becomes

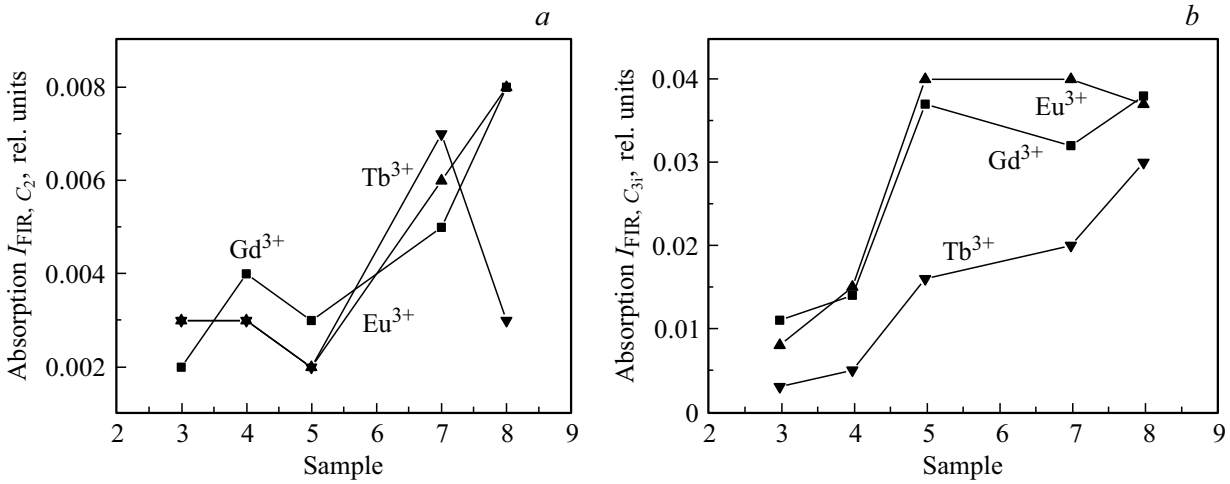

Figure 4. Intensities of FIR absorption bands, caused by cations motion in positions: C_2 (*a*) and C_{3i} (*b*).

questionable. It should be noted, that intensity of FL bands of monoclinic phase is the highest [3], probably as a result of removing restrictions on FL excitation transfer from Tb^{3+} ions to Eu^{3+} ions due to lack of different sublattices of C_{3i} and C_2. This is also contributed by increase of Ln^{3+} cations coordination number to 7.

Change of FIR spectra of sample 8 relative to sample 7 (Fig. 2, *4*), particularly increase of intensity of the band 141 cm^{-1} of Tb^{3+} ions and insignificant decrease of intensity of the band 122 cm^{-1} of Eu^{3+} ions in site C_{3i}, as well as decrease of intensity of the band 226 cm^{-1} of Tb^{3+} ions and increase of intensity of the band 208 cm^{-1} of Eu^{3+} ions in site C_2, confirm the facts of Tb^{3+} and Eu^{3+} cations distribution over the specified sites as per FL bands identification and increase of their intensity. This is with the exception of insignificant decrease of I_{FIR} value of the band 122 cm^{-1} of Eu^{3+} ions in position C_{3i}, that is caused by influence of Tamman effect, causing the crystal lattice loosening.

If dependencies of FIR bands intensities logically describe distribution of Eu^{3+} and Tb^{3+} ions over the centrosymmetric C_{3i} and the noncentrosymmetric C_2 sites, the redistribution of Gd^{3+} cations over the specified sites (Fig. 4) should have a logical explanation. As seen from Fig. 4, *b*, change of intensity of FIR bands of Gd^{3+} ions in site C_{3i} mirrors a change of specific surface of the crystallites (Fig. 1). The more complex dependence is observed for redistribution of Gd^{3+} ions in site C_2, that can be related to large amount of Tb^{3+} ions, transitioned after annealing of sample 3 in hydrogen from sites C_S into volume of crystallites of sample 4 (Fig. 4, *b*). At the same time, the substituted part of Gd^{3+} ions can transfer from sites C_{3i} to site C_2. The detailed analysis of these transitions nature is out of the scope of this work study.

It is known, that ratio of intensities of FL bands of Eu^{3+} ions 612/595 [nm] of radiative transitions $^5D_0 \rightarrow {}^7F_2$ and $^5D_0 \rightarrow {}^7F_1$, called asymmetric ratio AR, is related to concentration redistribution $AR = I_{612}/I_{595} = C_{24d}/C_{8b}$ of these ions over cation sites C_2 and C_{3i} [22–24]. This statement is sufficiently justified for C-Ln_2O_3 systems with one activator, e.g. Eu^{3+} at its low concentrations, when there are no exchange interactions between *f*-orbitals of these ions. Figure 3 shows a change of AR value depending on conditions of samples 3–8 formation. In the examined system with two FL activators of Tb^{3+} and Eu^{3+} such approach is unjustified. Indeed, from the table it follows, that samples 3 and 5 contain impurity phases Tb_7O_{12} : Eu^{3+} and $TbO_{1.81}$: Eu^{3+}, which also contain cation positions C_{3i}. This brings uncertainties in assessment of FL activators distribution over the specified phases and C-Gd_2O_3 matrix. From the other side, cations concentration in samples 7 and 8 is so high (2.5 mol%), that cross exchange interactions start between *f*-orbitals of both cations. In this system it results in equality disruption of ratios of FL bands intensities and concentrations of activators of $I_{C_2}/I_{C_{3i}} = N_{C_2}/N_{C_{3i}}$, particularly due to emission suppression or increase of intensity of individual radiative transitions [9].

Figure 5, *a* shows ratios of FL bands intensities of Tb^{3+} ions of samples 3–8, from which only for sample 4 the values of AR = 0.71 and 0.63 (table) can be taken as ratios of these ions concentrations in noncentrosymmetric and centrosymmetric sites, respectively.

Since these FL bands are doublet of the bands of radiative transition $^5D_4 \rightarrow {}^7F_6$ of Tb^{3+} ions with phonons participations and without them, the value of $AR_{Tb^{3+}} = AR_{Tb,551} + AR_{Tb,545} = 1.34$ can be taken. For Eu^{3+} cations (Fig. 3, table) of sample 3 the value of $(AR)_{Eu^{3+}} = (I_{C_2}/I_{C_{3i}})_{Eu^{3+}} = 2.6$.

It can be assumed, that FIR spectra are less sensitive to the presence of impurity phases of Tb_7O_{12} and $TbO_{1.81}$ in C-Gd_2O_3 matrix and to exchange interactions of *f*-electrons of Tb^{3+} and Eu^{3+} activators cations. Indeed, change of ratios $I_{FIR,C_2}/I_{FIR,C_{3i}}$ (Fig. 5, *b*) for samples 3–7 remains similar to a change of specific surface of crystallites boundaries, that mainly defines the ratio of Tb^{3+} ions and Eu^{3+} ions in sites C_2 and C_{3i}. However, it should be

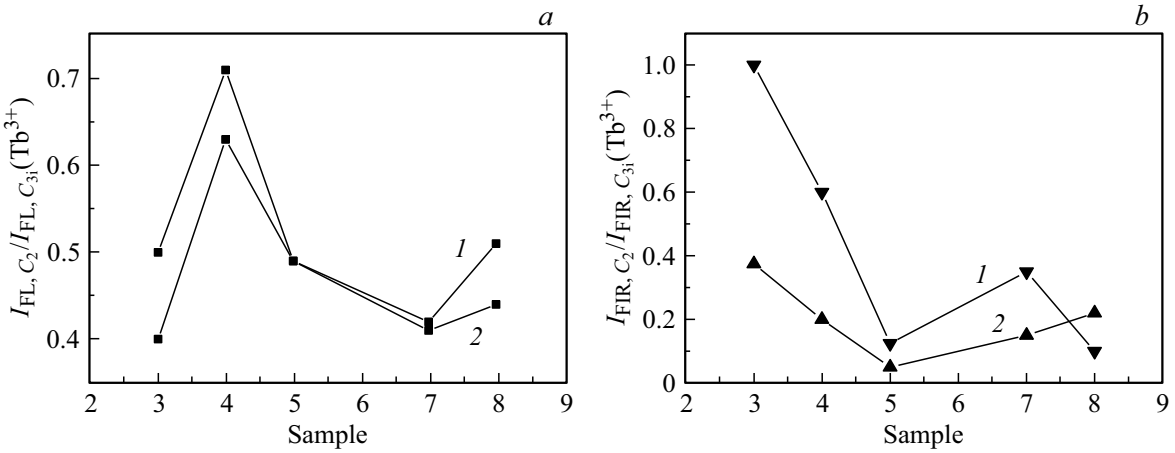

Figure 5. Change of ratios $I_{FL,C_2}/I_{FL,C_{3i}}$ of the bands 492/551 [nm] (*1*) and 492/545 [nm] (*2*) of Tb^{3+} ions (*a*), change of ratios $I_{FIR,C_2}/I_{FIR,C_{3i}}$ of Tb^{3+} (*1*) and Eu^{3+} (*2*) ions (*b*).

noted, that values of I_{FIR} are functions of force constants of cations and anions interactions and distances between them. Nature of these values change from one sample to another is unknown, but it can be assumed, that it does not strongly impact the values of I_{FIR} from sample to sample, since the similarity of dependencies S_{cr} and I_{FIR} remains for samples 3–7. This is indicated by the results of *X*-ray phase analysis and small changes of lattice parameter a (see the table). Sample 8 falls out of this series, probably due to the mentioned Tamman effect. Thus, the values of I_{FIR} can be considered as semi-quantitative assessment of Tb^{3+} and Eu^{3+} cations distribution over cation sites of C_2 and C_{3i} lattice of cubic matrix C-$Gd_2O_3:Tb^{3+},Eu^{3+}$.

4. Conclusion

The earlier proposed [14] option of FIR absorption bands of spectra 130 and 200 cm^{-1} of Eu^{3+} ions in cubic sesquioxides of Eu and Y consideration as markers of these ions location in C_{3i} and C_2 sites of bixbyite type lattice turned out to be rather productive for development of an algorithm for justification of two cations of FL activators distribution in a more complex system of C-$Gd_2O_3:Tb^{3+},Eu^{3+}$. As a results of the combined examination of changes of phase composition and samples morphology, as well as their FL and FIR spectra, the self-consistent data on centrosymmetric and noncentrosymmetric sites of cubic gadolinium sesquioxides lattice, as well as on surface states of C_S over crystallites boundaries were obtained. It was established, that modes of synthesis and annealing of samples of C-$Gd_2O_3:Tb_x,Eu_x$ ($x = 1.0$ and 2.5 mol%) at 900 and 1200°C in oxidizing air atmosphere and in reducing hydrogen atmosphere define, first of all, phase composition of the products and crystallites sizes. Change of these parameters is caused by transition of surface active terbium ions to the crystallites boundaries and coexistence of these ions in various degrees of oxidation of Tb^{3+} and Tb^{4+}. This, in its turn, is accompanied with inherent redistribution of FL activators over C_2 and C_{3i} to cation sites of the crystal lattice. At the same time, the FL spectra of the samples characteristically change. It is shown, that change of FL spectra of the samples correlates with a change of specific surface of crystallites and FIR spectra within known models of these spectra description. Using the obtained correlations of dependencies of S_{cr}, FL and FIR for Eu^{3+} cations on the modes of synthesis and annealing of the samples with known interrelations of FL bands with sites C_{3i} and C_2 of these ions localization, for the first time ever we expanded the understanding of such correlations nature to interpretation of interrelations of FL bands of Tb^{3+} cations 545, 551 and 492 nm with their localization by sites C_{3i} and C_2, respectively. The obtained results are required for creation of photoluminophores with a certain specified color due to controlled distribution of FL activators over crystal lattice with engagement of spectra analysis through considerably available FIR spectroscopy.

Funding

The work was supported by the Ministry of Science and Higher Education of the Russian Federation No. 121031700315-2.

Conflict of interest

The authors declare that they have no conflict of interest.

References

[1] A. Garcia-Murillo, A. de J. Morales Ramirez, F. de J. Carrillo Romo, M. Garcia Hernandez, M.A. Dominguez Crespo. Mater. Lett. **63**, 1631 (2009).
[2] S.V. Mahajan, J.H. Dickerson. Nanotechnology **18**, 325605 (2007).

[3] V.V. Bakovets, I.P. Dolgovesova, T.D. Pivovarova, M.I. Rakhmanova. FTT **62**, 2147 (2020) (in Russian).
[4] C.J. Shilpa, N. Dhananjaya, H. Nagabhushana, S.C. Sharma, C. Shivakumara, K.H. Sudheerkumar, B.M. Nagabhushana, R.P.S. Chakradhar. Spectrochim. Acta A **128**, 730 (2014).
[5] V.V. Bakovets, T.D. Pivovarova, I.P. Dolgovesova, I.V. Korol'kov, O.V. Antonova, S.I. Kozhemyachenko. ZhOKh **88**, 850 (2018) (in Russian).
[6] Z.K. Heiba, L. Arda, Y.S. Hascicek. J. Appl. Cryst. **38**, 306 (2005).
[7] V.V. Bakovets, E.S. Zolotova, O.V. Antonova, I.V. Korol'kov, I.V. Yushina. ZhTF **86**, 104 (2016) (in Russian).
[8] W.-C. Chien, Y.-Y. Yu, C.-C. Yang. Mater. Des. **31**, 1737 (2010).
[9] M. Nazarov, D.Y. Noh. J. Rare Earths **28**, 1 (2010).
[10] A. de J.M. Ramırez, A. Garcia Murillo, F. de J.C. Romoa, M.G. Hernandez, D.J. Vigueras, G. Chaderyron, D. Boyer. Mater. Res. Bull. **45**, 40 (2010).
[11] M.A. Flores-Gonzaleza, G. Ledouxa, S. Rouxa, K. Lebboua, P. Perriatb, O. Tillement. J. Solid State Chem. **178**, 989 (2005).
[12] V.V. Bakovets, A.V. Sotnikov, A.Sh. Agazhanov, S.V. Stankus, E.V. Korotaev, D.P. Pishchur, A.I. Shkatulov. J. Am. Ceram. Soc. **101**, 4773 (2018).
[13] R.P. Singh, K. Gupta, A. Pandey, A. Pandey. World J. Nano Sci. Eng. **2**, 1 (2012).
[14] D. Bloor, J.R. Dean. J. Phys. C **5**, 1237 (1972).
[15] P.P. Fedorov, M.V. Nazarkin, R.M. Zaklyukin. Kristallografiya **47**, 316 (2002) (in Russian).
[16] M.W. Urban, B.C. Cornilsen. J. Phys. Chem. Solids **48**, 475 (1987).
[17] N.T. Mcdevitt, A.D. Davison. J. Opt. Soc. Am. **56**, 636 (1966).
[18] Y. Repelin, C. Proust, E. Husson, M. Beny. J. Solid State Chem. **138**, 163 (1995).
[19] J. Ibanez, J.Á. Sans, V. Cuenca-Gotor, R. Oliva, Ó. Gomis, P. Rodrıguez-Hernandez, A. Munoz, U. Rodrıguez-Mendoza, M. Velazquez, P. Veber, C. Popescu, F.J. Manjon. Inorganic. Chem. **59**, 9648 (2020).
[20] H. Guo, X. Yang, T. Xiao, W. Zhang, L. Lou, J. Mugnier. Appl. Surf. Sci. **230**, 215 (2004).
[21] A. Ubbelode. Plavlenie i kristallicheskaya struktura. Mir, M. (1969). 420 p. (in Russian).
[22] J. Heber, K. H. Hellwege, U. Kobler, H. Murmann. Z. Physik **237**, 189 (1970).
[23] B. Antic, J. Rogan, A. Kremenovic, A.S. Nikolic, M. Vucinic-Vasic, D.K. Bozanic, G.F. Goya, P. Colomban. Nanotechnology **21**, 245702 (2010).
[24] R. Srinivasan, N.R. Yogamalar, J. Elanchezhiyan, R.J. Joseyphus, A.C. Bose. J. Alloy Compd. **496**, 472 (2010).